

Non-isothermal reduction kinetics of Fe₂O₃–NiO composites for formation of Fe–Ni alloy using carbon monoxide

Bo LI, Yong-gang WEI, Hua WANG

State Key Laboratory of Complex Nonferrous Metal Resources Clean Utilization,
Kunming University of Science and Technology, Kunming 650093, China

Received 10 December 2013; accepted 27 April 2014

Abstract: The non-isothermal reduction kinetics and mechanism of Fe₂O₃–NiO composites with different Fe₂O₃–NiO compacts using carbon monoxide as reductant were investigated. The results show that the reduction degree increases rapidly with increasing the content of NiO, and the presence of NiO also improves the reduction rate of iron oxides. It is found that NiO is preferentially reduced at the beginning of the reactions, and then the metallic Ni acts as a catalyst promoting the reduction rate of iron oxides. It is also observed that the increase of the NiO content enhances the formation of awaruite (FeNi₃) but decreases the percentage of kamacite (Fe,Ni) and taenite (Fe,Ni). The particle size of the materials tends to be uniform during the reduction process due to the presence of metallic nickel, metallic iron and the formation of Fe–Ni alloy. The concentration of CO in the product gas is greater than that of CO₂ at the beginning of the reaction and then slows down. The fastest reduction rate of Fe₂O₃–NiO composites with CO appears at 400–500 °C, and nucleation growth model can be used to elucidate the reduction mechanism. Nucleation growth process is found to be the rate controlling step when the temperature is lower than 1000 °C.

Key words: reduction kinetics; Fe₂O₃; NiO; Fe–Ni alloy; carbon monoxide

1 Introduction

The non-isothermal reduction of Fe₂O₃–NiO composites at low temperatures (≤ 1000 °C) is a pretreatment process of Fe₂O₃–NiO composites by carbon monoxide, which could improve the formation of Fe–Ni alloy. The investigation on the reduction kinetics of Fe₂O₃–NiO composites is very important for this process. The present investigations mainly focused on the reduction mechanism and reduction kinetics of iron oxide and nickel oxide [1–3]. ABDEL-HALIM et al [4] studied the carbothermic reduction kinetics of nanocrystallite Fe₂O₃–NiO composites for the formation of Fe–Ni alloy. Nanocrystalline compacts of pure and 26% NiO doped iron oxide were reduced at 800–1100 °C, and a continuous series of Fe–Ni alloy with different compositions were obtained. BAHGAT et al [5] investigated the reduction of WO₃–NiO–Fe₂O₃ and synthesis of nanocrystalline ternary W–Ni–Fe alloy [5]. Nanocrystalline 90%W–7%Ni–3%Fe alloy (mass

fraction) was synthesized through the gaseous reduction of WO₃–NiO–Fe₂O₃ mixture with pure hydrogen gas at 800–1000 °C. The effects of calcination temperature and doping with K₂O on the solid–solid interactions and physicochemical properties of NiO–Fe₂O₃ system were investigated using TG, DTA and XRD techniques. It was reported that Fe₂O₃ interacted readily with NiO to form crystalline NiFe₂O₄ phase at temperature from 700 °C. The degree of reaction propagation increased with increasing the calcination temperature [6]. JANKOVIC et al [7] studied the kinetics of non-isothermal nickel oxide reduction in hydrogen atmosphere using the invariant kinetic parameters method. The kinetics parameters (E_a , $\ln A$) were determined using Friedman (FR) isoconversional method and the invariant kinetic parameters method (IKP). The values of invariant kinetic parameters were used for numerical evaluation of conversion function. Thereafter, JANKOVIC et al [8] conducted the kinetic study of temperature-programmed reduction of nickel oxide in hydrogen atmosphere at four different heating rates. The kinetic model of the

Foundation item: Projects (51304091, U1302274) supported by the National Natural Science Foundation of China; Projects (2013FD009, 2013FZ007) supported by Applied Basic Research Program of Yunnan Province, China; Project (2012HB009) supported by the Candidate Talents Training Fund of Yunnan Province, China

Corresponding author: Hua WANG; Tel: +86-871-5153405; E-mail: wanghuaheat@hotmail.com
DOI: 10.1016/S1003-6326(14)63519-6

investigated reduction process was determined, and this model was corresponded to the empirical two-parameter Sestak–Berggren equation which gave a more quantitative description. The kinetic triplet obtained for the investigated process was $E_0=90.8$ kJ/mol, $\ln A=19.50$ and $f(\alpha)=\alpha^{0.63}(1-\alpha)^{1.39}$.

Based on the facts given above, the reduction kinetics and mechanism of $\text{Fe}_2\text{O}_3\text{-NiO}$ composites, which were obtained by thermal analysis method, were investigated by non-isothermal reduction with carbon monoxide at the atmospheric pressure in the present work. The present study is designated to prepare Fe–Ni alloy from different proportions of pure metal oxides. Reduction by carbon monoxide was investigated in binary system oxide ($\text{Fe}_2\text{O}_3\text{-NiO}$) and the obtained results will be used for the production of Fe–Ni alloy from pure metal oxides or nickel laterite ore.

2 Experimental

The reduction behavior of the prepared samples was investigated by thermo-gravimetric technique and effluent gas analysis method to measure the total mass loss of oxygen as a function of time and the component of outlet gases, respectively. The experiments were carried out in a self-made experimental platform, as shown in Fig. 1, and the quartz basket was hanged on the balance and settled in the middle zone of the tube furnace. The samples were reduced directly within the thermobalance, in korund pans, under 99.95% carbon monoxide (volume fraction) flowing at the rate of 100 mL/min with the heating rates of 10 °C/min in the temperature range from room temperature to 1000 °C. The mass of sample used for thermogravimetric investigations was about 5 g. The mass loss was recorded using an automatic sensitive electronic balance.

Since thermo-gravimetric technique offers only the general behavior of reduction processes by measuring the total mass loss of oxygen, gas chromatography (Agilent 6890N) and X-ray diffraction (Japan Science D/max-R diffractometer) techniques were used to measure the concentration of CO and CO_2 in the outlet gas and phase changes during the reduction, respectively, for the further discussion on the reduction mechanism. For XRD measurement, the X-ray tube was operated at 40 kV and 200 mA, and the X-ray diffractogram was recorded at 0.01° intervals with a scanning rate of 10 (°)/min for the scanning angle (2θ) from 10° to 90°. The morphology and particle size were determined using scanning electron microscopy (SEM) on a Philip XL30 scanning electron microscope. The degree of reduction was calculated by the changes of oxygen content in the sample.

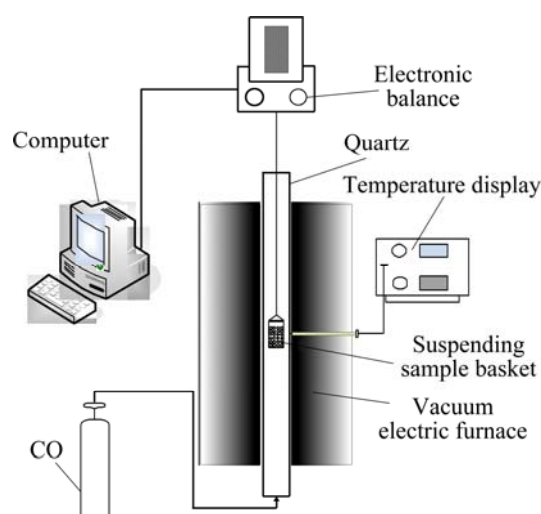


Fig. 1 Schematic diagram of self-made experimental platform

3 Results and discussion

3.1 Reducibility of metal oxides with carbon monoxide

The reduction behavior of three different proportions of nanosized materials, namely $\text{Fe}_2\text{O}_3\text{-NiO}$ compacts, was investigated. Firstly, the reducibility of three compacts was tested in thermo-gravimetric apparatus. The general trend of reduction process for the three compacts non-isothermally reduced is shown in Fig. 2. It can be observed that the mass loss is greatly affected by reduction temperature. Increasing reduction temperature from 400 to 900 °C causes the increase of the mass loss. All the three compacts failed to attain complete mass loss, and 75.9%, 75.6% and 78.9% mass losses were obtained for the $w(\text{Fe}_2\text{O}_3)/w(\text{NiO})=1:2$; 1:1; 2:1 compacts, respectively. This can be attributed to the formation of dense metallic layer and the difficulty of gas–solid state reduction of lower iron oxides at low reduction temperature.

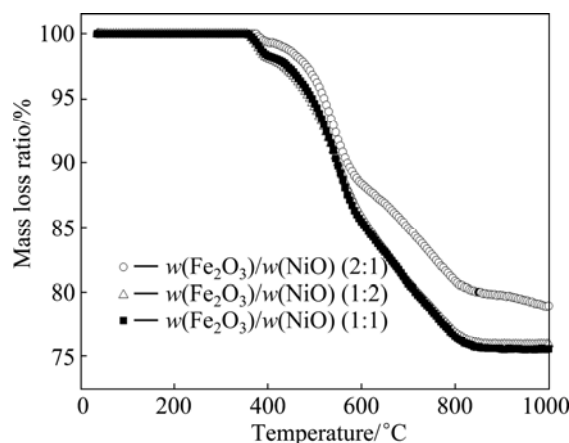


Fig. 2 Mass loss of different compacts reduced with carbon monoxide in temperature of 25–1000 °C

Figure 3 shows the reaction fraction of the different proportion compacts reduced by carbon monoxide. It can be seen that the reduction degree has no significant change as the reduction temperature increased both at the initial and final reaction stages. For each reduction reaction fraction curve, the reduction rate is the highest at early stages and gradually decreases with increasing time till the end of the experiment. It is also noticed that the increase of the NiO content results in higher reduction rate for the three samples, indicating that nickel species play a considerable role in the reduction of the mixed oxides and greatly affect the morphological changes accompanying reduction process. It is reported that NiO was firstly reduced, and then the metallic Ni could act as a catalyst promoting the reduction rate of iron oxides [4,9]. This can be used to explain the increased reduction rate of the samples with relatively higher NiO content, as observed above.

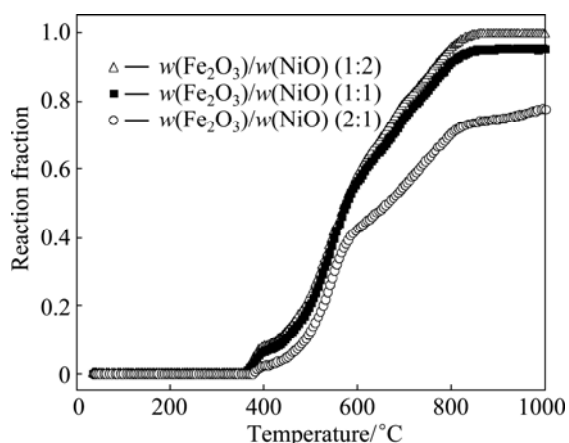


Fig. 3 Reaction fraction of different proportion compacts reduced with carbon monoxide in temperature of 25–1000 °C

Figure 4 shows the XRD pattern of different proportion compacts reduced. XRD analysis indicates that awaruite (FeNi_3), kamacite (Fe,Ni) and taenite (Fe,Ni) are the crystalline phases of the reduced samples, and metallic nickel and metallic iron phases are detected. As the mass ratio of Fe_2O_3 to NiO is 1:2, the crystalline phase is awaruite (FeNi_3). Increasing the content of NiO causes the increase in the mass fraction of awaruite (FeNi_3) and the decrease in the mass fraction of kamacite (Fe,Ni) and taenite (Fe,Ni). Thus, it can be found that increasing the content of NiO enhances the crystalline phases of the reduced compacts.

The microstructures of the compacts reduced were examined by SEM, as shown in Fig. 5. The three samples showed similar internal structures, and the granular structures were observed when the reduction process was completed. Comparatively at higher content of NiO, the grain growth of Fe–Ni alloy was observed on the composite particles that was more deformed forming

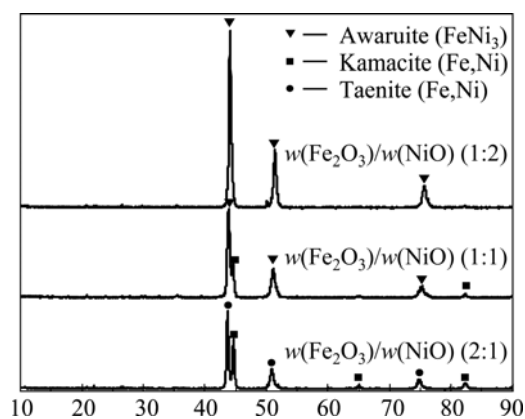


Fig. 4 XRD patterns of different proportion compacts reduced

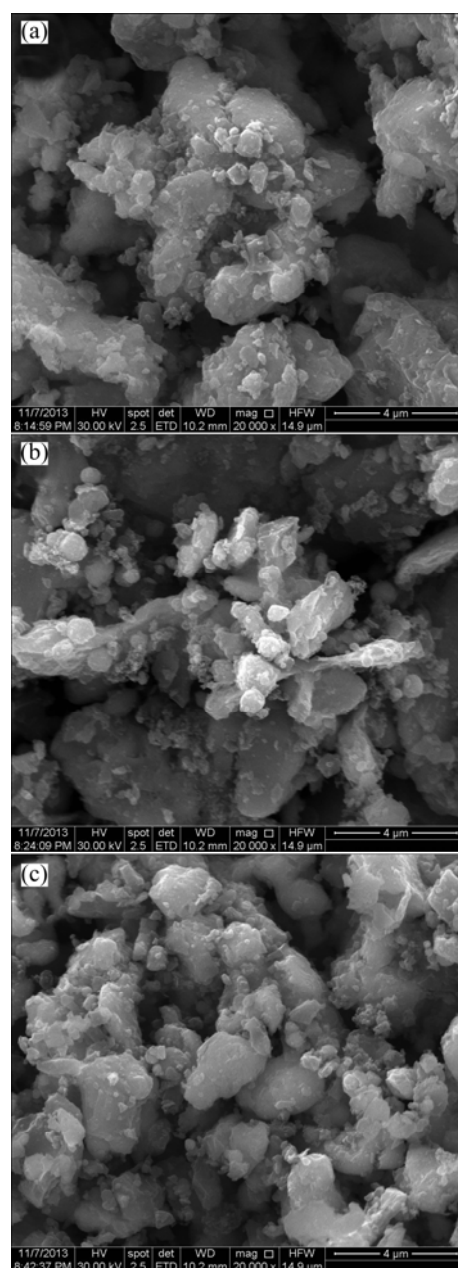
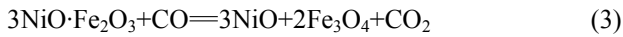


Fig. 5 SEM images of reduced compacts with different mass ratio of Fe_2O_3 to NiO: (a) 1:1; (b) 1:2; (c) 2:1

dense structure [5]. But the symmetrical size of particles may be attributed to the presence of metallic nickel and metallic iron, and the formation of Fe–Ni alloy [10,11].

3.2 Reduction mechanisms and kinetics

For the reduction process of metal oxides in carbon monoxide atmosphere, the reduction reactions can be expressed as follows [12]:



In the solid state reduction process of metal oxides, the reaction between $\text{Fe}_2\text{O}_3/\text{NiO}$ and carbon monoxide belongs to gas–solid reaction. Based on the reduction of trevorite ($\text{NiO} \cdot \text{Fe}_2\text{O}_3$), the preferential reduction of nickel oxide to metallic nickel can occur as Eqs. (3)–(5), and the further reduction of wustite to metallic iron takes place as Eq. (6).

The variation of gas composition of CO and CO_2 in the product gas can be used to discuss the mechanism of the reaction, as shown in Fig. 6. The CO diffuses and reacts with oxides to generate more CO_2 . It can be observed that the concentration of CO is greater than that of CO_2 at the beginning of the reaction and then slows down [13,14]. The minimum concentration of CO as well as the maximum concentration of CO_2 appear at 400–500 °C, which suggests that the reduction rate of $\text{Fe}_2\text{O}_3\text{–NiO}$ with CO is the fastest at this temperature range, namely the maximum reduction rate. It is known that the reduction reaction of iron oxides precedes in a stepwise manner ($\text{Fe}_2\text{O}_3 \rightarrow \text{Fe}_3\text{O}_4 \rightarrow \text{FeO} \rightarrow \text{Fe}$). The reduction products of $\text{Fe}_2\text{O}_3\text{–NiO}$ compacts have the equilibrium transformations $\text{Fe}_3\text{O}_4\text{–FeO}$ and NiO–Ni at the initial stage of reduction, and FeO–Fe equilibrium conversion is obtained at the final reaction stages.

The results obtained can be used for analyzing kinetic data and elucidating the mechanism of reduction of metal oxides by carbon monoxide. Compared with the nucleation growth model, the interfacial reaction model and the Coats–Redfern model, the nucleation growth model has a maximum linear correlation. Based on the maximum correlation coefficient, the nucleation growth model can be used to elucidate the reduction mechanism. The mathematical model of the kinetics of nucleation growth is expressed as follows [15,16]:

$$\ln \left[\left(\frac{\alpha}{1-\alpha} \right) / T^2 \right] = \ln \left[\frac{4\pi r_0^3 AR}{3\beta E} \left(1 - \frac{2RT}{E} \right) \right] - \frac{E}{RT} \quad (7)$$

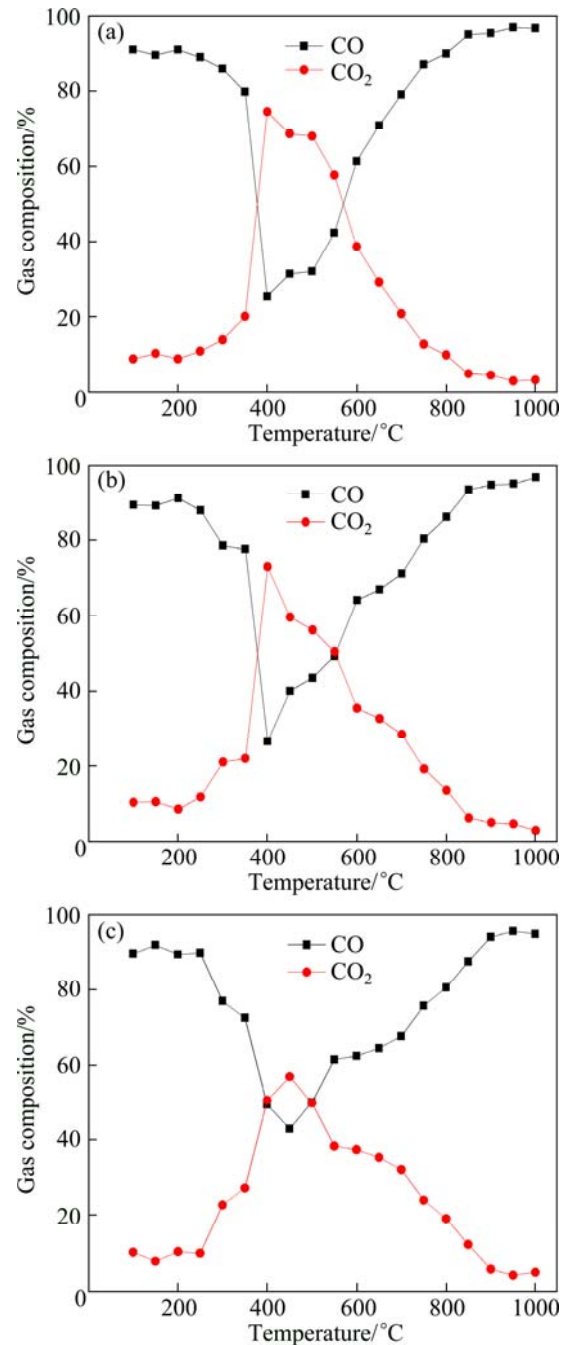


Fig. 6 Variation of composition of CO and CO_2 in product gas with increasing temperature for samples with different $w(\text{Fe}_2\text{O}_3)/w(\text{NiO})$: (a) 1:2; (b) 1:1; (c) 2:1

where α is the reaction fraction of reduction; A is the pre-exponential factor; E is the apparent activation energy; β is the reaction rate constant; R is the gas constant; r_0 corresponds to the radii of the solid grains at temperature of T_0 .

According to the reaction fraction of the different proportion compacts in Fig. 3, the relationship curves of $\ln[\alpha \cdot (1-\alpha)^{-1} \cdot T^2]$ and $1/T$ for the different proportions compacts are shown in Figs. 7–9. The results of this analysis can be obtained by Eq. (7) in Figs. 7–9. The

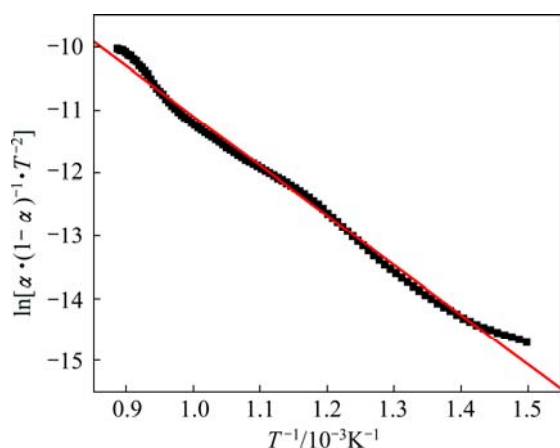


Fig. 7 Plot of $\ln[\alpha \cdot (1-\alpha)^{-1} \cdot T^{-2}]$ versus $1/T$ for $\text{Fe}_2\text{O}_3/\text{NiO}(1:2)$

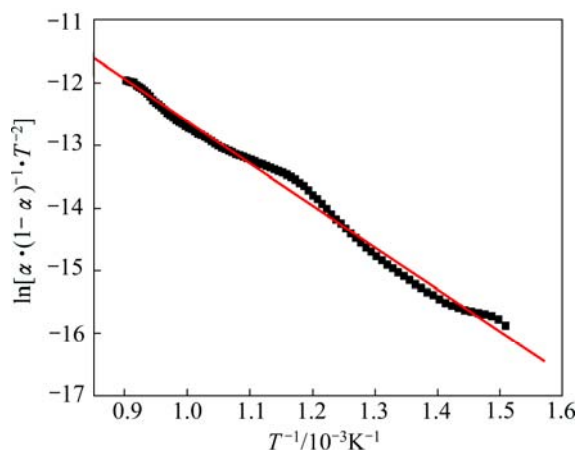


Fig. 8 Plot of $\ln[\alpha \cdot (1-\alpha)^{-1} \cdot T^{-2}]$ versus $1/T$ for $\text{Fe}_2\text{O}_3/\text{NiO}(1:1)$

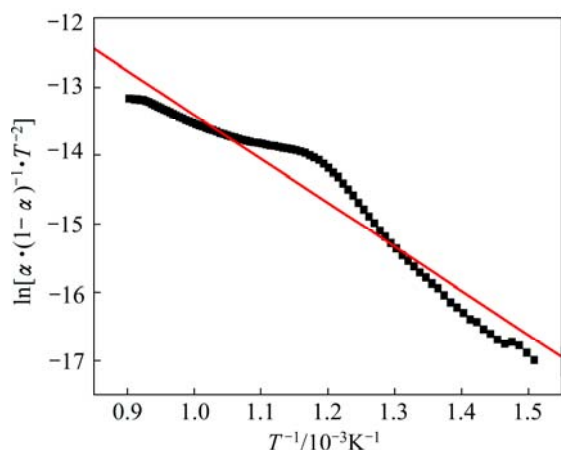


Fig. 9 Plot of $\ln[\alpha \cdot (1-\alpha)^{-1} \cdot T^{-2}]$ versus $1/T$ for $\text{Fe}_2\text{O}_3/\text{NiO}(2:1)$

related coefficients of the lines in Figs. 7–9 are 0.996, 0.995 and 0.970, respectively.

The curves of the different proportion compacts reduction reactions were approximately linear, and the apparent activation energies E and pre-exponential factors A can be calculated using slope and intercept [17,18]. The apparent activation energies and pre-exponential factors of the different proportion

compacts reduction reactions are listed in Table 1. Compared with the calculated values of apparent activation energies for $\text{Fe}_2\text{O}_3/\text{NiO}(1:1)$ and $\text{Fe}_2\text{O}_3/\text{NiO}(2:1)$, the apparent activation energy of $\text{Fe}_2\text{O}_3/\text{NiO}(1:2)$ is the maximum value, and pre-exponential factor increases with increasing of apparent activation energy. It is observed that gas–solid reaction seems to have an effect particularly at the initial stage [19].

Table 1 Apparent activation energies E and pre-exponential factors A at different proportions compacts reduction reactions

Mass ratio of Fe_2O_3 to NiO	$E/(\text{kJ}\cdot\text{mol}^{-1})$	$A/(\text{s}^{-1}\cdot\text{cm}^{-3})$
1:2	68.27	1909790
1:1	65.97	106626
2:1	53.38	33479

4 Conclusions

1) The reduction degree increases rapidly with increasing the content of NiO in Fe_2O_3 –NiO composites, indicating that Ni species play a considerable role in the reduction process of the mixed oxides. It is found that the NiO is firstly reduced, and then the metallic phase of Ni can act as a catalyst, promoting the reduction rate of iron oxides.

2) Increasing the content of NiO can improve the formation of awaruite (FeNi_3) but restrain the generation of kamacite (Fe,Ni) and taenite (Fe,Ni). Thus, it can be reported that the content of NiO enhanced the crystalline phases of the compacts reduced. The symmetrical size of particles may be attributed to the presence of metallic nickel and metallic iron and the formation of Fe–Ni alloy.

3) The concentration of CO in the product gas is greater than that of CO_2 at the beginning of the reaction and then slows down. The minimum concentration of CO as well as the maximum concentration of CO_2 appears at 400–500 °C, which suggests that the maximum reduction rate of $\text{Fe}_2\text{O}_3/\text{NiO}$ appears at this temperature stage.

4) Based on the maximum correlation coefficient, the nucleation growth model can be used to elucidate the reduction mechanism. Nucleation growth process is the major rate controlling step particularly at the reaction temperatures (≤ 1000 °C). The calculated values of apparent activation energy reveal that gas–solid reaction control seems to have an effect particularly at the initial reaction stage.

References

- [1] WEN Fei, WANG Hui, TANG Zong-xue. Kinetic study of the redox process of iron oxide for hydrogen production at oxidation step [J].

- Thermochimica Acta, 2011, 520: 55–60.
- [2] ADNADEVIC B, JANKOVIC B. Dispersive kinetic model for the non-isothermal reduction of nickel oxide by hydrogen [J]. Physica B, 2008, 403: 4132–4138.
- [3] HE Fei-jiao, Yang Juan, LEI Tong-xin, GU Chun-yan. Structure and properties of electrodeposited Fe–Ni–W alloys with different levels of tungsten content: A comparative study [J]. Applied Surface Science, 2007, 253: 7591–7598.
- [4] ABDEL-HALIMA K S, KHEDRB M H, NASRA M I, ABDEL-WAHABB M S H. Carbothermic reduction kinetics of nanocrystallite Fe₂O₃/NiO composites for the production of Fe/Ni alloy [J]. Journal of Alloys and Compounds, 2008, 463: 585–590.
- [5] BAHGAT M, PAEK M K, PAK J J. Reduction investigation of WO₃/NiO/Fe₂O₃ and synthesis of nanocrystalline ternary W–Ni–Fe alloy [J]. Journal of Alloys and Compounds, 2009, 472: 314–318.
- [6] SHAHEEN W M. Thermal solid–solid interactions and physicochemical properties of NiO/Fe₂O₃ system doped with K₂O [J]. Thermochimica Acta, 2008, 470: 18–26.
- [7] JANKOVIC B, ADNADEVIC B, MENTUS S. The kinetic analysis of non-isothermal nickel oxide reduction in hydrogen atmosphere using the invariant kinetic parameters method [J]. Thermochimica Acta, 2007, 456: 48–55.
- [8] JANKOVIC B, ADNADEVIC B, MENTUS S. The kinetic study of temperature-programmed reduction of nickel oxide in hydrogen atmosphere [J]. Chemical Engineering Science, 2008, 63: 567–575.
- [9] ZHANG Y, WEI W, YANG X, WEI F. Reduction of Fe and Ni in Fe–Ni–O systems [J]. Journal of Mining and Metallurgy, Section B: Metallurgy, 2013, 49: 13–20.
- [10] LI Bo, WANG Hua, WEI Yong-gang. The reduction of nickel from low-grade nickel laterite ore using a solid-state deoxidation method [J]. Minerals Engineering, 2011, 24: 1556–1562.
- [11] ZHANG Chuan-fu, YAO Yong-lin, ZHANG Yin-liang, ZHAN Jing. Preparation of ultra-fine fibrous Fe–Ni alloy powder by coordinated co-precipitation–direct reduction process [J]. Transactions of Nonferrous Metals Society of China, 2012, 22: 2972–2978.
- [12] OLLI A, LAURI H, PETER P. Nickel ore reduction by hydrogen and carbon monoxide containing gases [J]. Mineral Processing and Extractive Metallurgy Review, 1995, 15: 169–179.
- [13] LI Bo, WANG Hua, WEI Yong-gang. The kinetic analysis for non-isothermal solid state reduction of nickel laterite ore by carbon monoxide [J]. Mineral Processing and Extractive Metallurgy, 2012, 121: 178–184.
- [14] ABDEL-HALIM K S, BAHGAT M, FOUAD O A. Thermal synthesis of nanocrystalline FCC Fe–Ni alloy by gaseous reduction of coprecipitated NiFe₂O₄ from secondary resources [J]. Materials Science and Technology, 2006, 22: 1396–1400.
- [15] TAO Dong-ping. Mathematical models of the kinetics of dynamic thermogravimetry [J]. Thermochim Acta, 1989, 145: 165–172.
- [16] TAO Dong-ping, YANG Xian-wan. Kinetics of disproportionation and reduction of stannous oxide and mechanism of reduction of stannous oxide [J]. The Chinese Journal of Nonferrous Metals, 1998, 8: 126–130. (in Chinese)
- [17] HUA Yi-xin. Kinetics of reactions in metallurgical processes [M]. Beijing: Metallurgical Industry Press, 2004. (in Chinese)
- [18] HU Rong-zu, GAO sheng-li, ZHAO Feng-qi, SHI Qi-zhen, ZHANG Tong-lai, ZHANG Jian-jun. Thermal analysis kinetics [M]. Beijing: Science Press, 2008. (in Chinese)
- [19] ABDEL-HALIM K S. Isothermal reduction behavior of Fe₂O₃/MnO composite materials with solid carbon [J]. Materials Science and Engineering A, 2007, 452–453: 15–22.

CO 还原 Fe₂O₃–NiO 复合物形成 Fe–Ni 合金的非等温还原动力学

李 博, 魏永刚, 王 华

昆明理工大学 省部共建复杂有色金属资源清洁利用国家重点实验室, 昆明 650093

摘 要: 研究采用 CO 还原不同比例 Fe₂O₃–NiO 复合物的非等温还原动力学及机理。结果表明: 随着 NiO 含量的增加, 样品的还原程度不断提高, NiO 的存在提高氧化铁还原率。在还原开始阶段, NiO 优先被还原, Ni 作为催化剂可以提高氧化铁的还原率。NiO 含量的增加促进镍铁相(FeNi₃)的增加, 但导致铁纹石相(Fe₃Ni)和镍纹石相(Fe₂Ni)的减少。金属镍、金属铁及镍铁合金的形成导致微观颗粒具有均匀性。在还原初始阶段, 气体产物中 CO 浓度大于 CO₂ 浓度, 然后逐渐减小, 当温度在 400~500 °C 内, Fe₂O₃–NiO 复合物的还原速率达到最大值, 成核长大模型可以揭示还原机理。在温度低于 1000 °C 的条件下, 成核长大过程是还原反应速率的限制环节。

关键词: 还原动力学; Fe₂O₃; NiO; Fe–Ni 合金; CO

(Edited by Chao WANG)